ISPRS Journal of Photogrammetry and Remote Sensing 226 (2025) 102–115

Contents lists available at ScienceDirect

ISPRS Journal of Photogrammetry and Remote Sensing

journal homepage: www.elsevier.com/locate/isprsjprs

Combining optical and SAR satellite data to monitor coastline changes in the Black Sea

Dalin Jiang [a,*], Armando Marino [a], Maria Ionescu [b,c,*], Mamuka Gvilava [d], Zura Savaneli [e], Carlos Loureiro [f,g], Evangelos Spyrakos [a], Andrew Tyler [a], Adrian Stanica [b]

[a] Earth and Planetary Observation Sciences (EPOS), Biological and Environmental Sciences, Faculty of Natural Sciences, University of Stirling, Stirling, United Kingdom
[b] National Institute of Marine Geology and Geo-ecology (GeoEcoMar), Bucharest, Romania
[c] Faculty of Geology and Geophysics, University of Bucharest, Bucharest, Romania
[d] GIS and RS Consulting Center GeoGraphic, Tbilisi, Georgia
[e] Tbilisi State University, Tbilisi, Georgia
[f] Centre for Marine and Environmental Research (CIMA/ARNET), Faculty of Science and Technology, Universidade do Algarve, Faro, Portugal
[g] Geological Sciences, School of Agricultural, Earth and Environmental Sciences, University of KwaZulu-Natal, Durban, South Africa

ARTICLE INFO

Keywords:
Black Sea
Coastline
Erosion
Artificial shorelines
Earth observation

ABSTRACT

The coastal environments of the Black Sea are of high ecological and socio-economic importance. Understanding changes along this extensive and complex coastline can help us comprehend the pressures from nature, society, and extreme events, providing valuable insights for more effective management and the prevention of future adverse changes. Current methods for monitoring coastal dynamics rely on the accurate extraction of coastlines from optical and/or Synthetic Aperture Radar (SAR) images, providing information only on the rate of change. This study developed a simple yet novel approach by combining Sentinel-1 SAR image for surface change detection and Sentinel-2 Multispectral Instrument (MSI) optical image for coastline detection, which provides data on both the rate and area of change. Coastlines were extracted from the Modified Normalised Difference Water Index (MNDWI) calculated from MSI images and rates of change were calculated from the extracted coastlines. SAR images for the same areas were stacked and differences during the analysis period were calculated, allowing the determination of the area of change. Another new method was developed to combine the changes detected from optical and SAR images, and only results in locations showed consistent change direction (erosion or accretion) were retained. The extracted coastlines were validated using *in situ*-measured coastlines along the Romanian and Georgian coasts. The validation analysis showed that the average difference between satellite-derived and *in situ* coastlines was 11.8 m. The method developed was then applied to the entire Black Sea coast, revealing 35.1 km^2 of changes between 2016 and 2023. These observed changes include 23.9 km^2 (68 %) coastal advance and 11.3 km^2 (32 %) of retreat. A total of 54 % of the changes are estimated to be the result of natural coastline erosion or accretion, whilst 35 % can be attributed to artificial changes related to construction activity. Around 11 % are attributed to random occurrences due to boat/ship movement or land cover changes on adjacent land. Natural coastline changes were mainly observed in the vicinity of deltaic and estuarine system and along sandy shorelines, including along the Danube Delta, Kızılırmak-Yeşilırmak deltas, Chorokhi-Rioni-Kodori River mouths and the coast from Dnieper-Bug Estuary to Karkinit Bay. Artificial changes were mainly found along the southern Black Sea coast, where airports, ports, harbours, and jetties have been constructed in recent years. The proposed method provides a simple, efficient and accurate way for coastline change monitoring, and findings in this study can support the sustainable coastal zone management in the Black Sea.

* Corresponding authors at: Earth and Planetary Observation Sciences (EPOS), Biological and Environmental Sciences, Faculty of Natural Sciences, University of Stirling, Stirling, United Kingdom (D. Jiang); National Institue of Marine Geology and Geo-ecology (GeoEcoMar), Bucharest, Romania (M. Ionescu)
E-mail addresses: dalin.jiang@stir.ac.uk (D. Jiang), maria.ionescu@geoecomar.ro (M. Ionescu).

https://doi.org/10.1016/j.isprsjprs.2025.05.003
Received 14 October 2024; Received in revised form 19 April 2025; Accepted 5 May 2025
Available online 15 May 2025

1. Introduction

Coastal zones are one of the most diverse, productive and populated areas (McLean et al., 2001). It is estimated that around 37 % of the global population lives within 100 km from the coastline (Cohen et al., 1997). Marshes, wetlands, lagoons, estuaries, beaches and river deltas in coastal zones are important habitats for birds, fishes and other wildlife, and provide essential ecosystem services to human society (Barbier et al., 2011; Luisetti et al., 2014; Newton et al., 2018). However, coastal zones face significant threats from sea level rise, storms, floods, and anthropogenic disturbance (Edmonds et al., 2020; Nicholls et al., 2021). A growing population and intensifying climate change, including more frequent extreme weather events and accelerating rising sea levels, amplify these threats (Nicholls and Cazenave, 2010; IPCC, 2021; UN, 2022). These can lead to, or accelerate, the loss of beach, destruction of habitats, reduction of productivity, drive biodiversity declines, and impact settlements in coastal zones (Michener et al.,1997; Nicholls and Cazenave, 2010; Hauer et al., 2020; Hooijer and Vernimmen, 2021). The sustainable management of coastal zones, therefore requires the monitoring of coastline change and a better understanding of their spatio-temporal patterns, which in turn will enable the stability or vulnerability of coastal areas to be established.

Coastline change monitoring at regional to global scales requires datasets with extensive spatial and temporal coverage, as well as sufficient detail to capture changes on the order of a few metres. Satellite-based Earth Observation (EO) provides an efficient way for monitoring coastline changes due to its large synoptic spatial coverage, short revisit period, and relatively long historical imagery archives (Luijendijk et al., 2018; Mentaschi et al., 2018). Generally, there are two types of spaceborne EO data that can be used for coastline change monitoring (Apostolopoulos and Nikolakopoulos, 2021). The first, optical imagery, enables coastlines to be extracted by calculating index such as the Normalised Difference Water Index (NDWI) (Ghosh et al., 2015; Yasir et al., 2020; Bishop-Taylor et al., 2021; Görmüş et al., 2021), image classification tools (Sekovski et al., 2014; Vos et al., 2019; Scala et al., 2024), machine learning models (Seale et al., 2022; Fogarin et al., 2023), or combining some of those approaches. The advantage of optical imagery is that it can clearly distinguish water and land because of the high land reflectance and low water reflectance. However, it can be influenced by clouds, shadows of clouds, buildings and mountains, and reflection from sea floor and adjacent land (Feyisa et al., 2014; Jiang et al., 2023). The second type of data is Synthetic Aperture Radar (SAR) imagery, from which coastlines can be extracted using segmentation methods (Niedermeier et al., 2000; Modava et al., 2018; Ciecholewski, 2024), and coastline changes can be detected by comparing the extracted coastlines at different times. The advantage of SAR imagery is that it is not affected by weather conditions (e.g., cloud or fog) and is good at target detection (Tsokas et al., 2022; Yasir et al., 2024). However, the effectiveness of SAR data for coastline extraction can be influenced by flat surfaces such as mudflat or fine sand beaches, because their low backscattering is very similar to the one from surface water. Some studies have tried to combine optical and SAR data for coastline change monitoring (e.g., Zhu et al., 2021; Paz-Delgado et al., 2022; Bar et al., 2024; Mao and Splinter, 2025), but they mainly used SAR as an addition to optical data for coastline extraction. The consistency between coastlines extracted from these two types of data need more investigation, and the effectiveness of SAR for surface objects and change detection have not been fully used yet. Therefore, developing an approach by using the advantages of optical imagery for water-land differentiation and SAR imagery for surface change detection will be very useful for coastline change monitoring.

The coastal zones of the Black Sea are experiencing various stressors mainly due to human interventions, both directly along the coasts and indirectly by reducing sediment supply, as well as from the impacts of sea level rise, change in wind and wave conditions, intensified extreme events, all of which leading to detrimental consequences such as loss of beaches, land, or damage to infrastructure and buildings (Karsli et al., 2011; Allenbach et al., 2015; Kosyan and Velikova, 2016; Aydoğan and Ayat, 2018; Goksel et al., 2020; Vilibić et al., 2021; Giosan et al., 1999; Ungureanu and Stanica, 2000; Panin, 2005; Stanica et al., 2007; Abaza et al., 2011; Avşar and Kutoğlu, 2020). Many studies have been conducted on the Black Sea coast, focusing on various aspects of coastal dynamics including assessing coastline change to understand coastal processes (Giosan et al., 1999; Panin, 2005; Stanica and Panin, 2009). However, most of these studies rely on direct measurements of the coastal geomorphological parameters, and topographic and bathymetric maps. More recently, studies based on EO have been carried out to monitor coastline change of the Black Sea (Karsli et al., 2011; Stanchev et al., 2018; Kale et al., 2019; Goksel et al., 2020; Medinets et al., 2022), but most of them focused on relatively small areas. For example, Ozturk and Sesli (2015) studied the coastline changes in Kızılırmak Delta using topographic maps (1962) and Landsat images (1974, 1987 and 2013), indicating maximum erosion along the coasts of the delta of −827 m, and the total area of change between 1962 and 2013 was 963 ha. At the basin scale, the recent work by Görmüş et al. (2021) considered coastline changes in the Black Sea from 1972 to 2018 using the Landsat imagery archive. Görmüş' approach relied on the use of only 3–8 optical satellite images per coastline sector over the ~ 40 years of analysis, leaving large temporal gaps between images used to investigate coastline changes. Given the increasing population, intensifying extreme events and expanding economic activities in the Black Sea, and crucially the increased availability of recently launched satellites (e.g., Sentinel-2 in 2015), providing higher spatial and temporal resolutions, new basin-wide insights into coastline change characteristics can now be realised.

This study therefore aims to: (1) develop a new and simple method to detect coastline changes combining Sentinel optical and SAR images; (2) evaluate the accuracy and validate the developed method using *in situ*-measured coastline data in sectors of the Black Sea; and (3) apply the developed method to the entire Black Sea coast to monitor coastline changes between 2016 and 2023.

2. Methodology

2.1. Study area

This study focuses on the entire Black Sea coast (excluding Sea of Azov, Fig. 1), which is a semi-enclosed sea bordered by Bulgaria, Georgia, Romania, Russian Federation, Turkey and Ukraine. The main rivers flowing into the Black Sea are the Danube, Dniester, Dnieper and Bug rivers located in the west and north-west. These rivers cover 82 % of the total Black Sea catchment area and contribute to approximately 76 % of the total freshwater flow into the Black Sea. The largest and most significant river is the Danube River, whose basin covers 44 % of the entire Black Sea catchment (Vespremeanu and Golumbeanu, 2017). The Danube's influence is particularly significant for sedimentation on the north-western Black Sea coast and shelf area. Its influence reaches far south to the Bosphorus region and down to the deep-sea floor (Panin and Jipa, 2002). The Black Sea coast can be categorised into three main types: low and accretionary coasts, erosive sedimentary coasts, and rocky mountainous coasts (Panin, 2005). The topography of the western and north-western coasts is relatively flat, while the southern and south-western coasts are bordered by the Balkan Mountains, and the eastern and north-eastern coasts by the Caucasus Mountains (Panin, 2005; Tătui et al., 2019). The Black Sea has complex current patterns, driven by atmospheric circulation, wind, river discharge, and density differences, rather than tides. These currents are influenced by the shape of the coastline, underwater topography, and coastal structures like jetties. The sea's basin shape creates two large eddies in the west and east, as well as a rim current around the entire basin (Halcrow, 2012).

Fig. 1. Map of the study area. Blue lines represent rivers, the black solid line indicates the studied coastline in the Black Sea, black boxes with dashed line mark the location where *in situ* coastline were measured, colour of the background indicates the elevation. River and elevation data were sourced from HydroSHEDS (Lehner et al., 2008) and the General Bathymetric Chart of the Oceans (GEBCO), respectively. (For interpretation of the references to colour in this figure legend, the reader is referred to the web version of this article.)

2.2. Satellite data collection and processing

To define the area for analysis, a 1 km buffer around the entire Black Sea coast was created based on the coastline location obtained from the European Environment Agency (https://www.eea.europa.eu). This 1 km buffer zone along the Black Sea coast was used to download and crop the satellite images. All further analysis of coastal dynamics were undertaken within this buffer zone.

2.2.1. Optical image processing

We downloaded Sentinel-2 MultiSpectral Instrument (MSI) Level-1 top-of-atmosphere (TOA) reflectance images for the months of July and August between 2016 and 2023 within the 1 km buffer using Google Earth Engine (GEE). The spatial resolution of the MSI is 20 m, and only scenes with cloud cover less than 10 % were used. The median of TOA reflectance image in July and August in each year were calculated to obtain yearly cloud-free images for the entire Black Sea coast. We then calculated the Modified Normalised Difference Water Index (MNDWI, Xu, 2006) from the median TOA reflectance image for each year:

$$\mathrm{MNDWI} = \frac{B_3 - B_{11}}{B_3 + B_{11}} \quad (1)$$

where B_3 and B_{11} are the TOA reflectance of green (560 nm) and short-wave infrared (SWIR, 1614 nm) bands from MSI, respectively. MNDWI was chosen because of its simplicity and efficiency in land–-water differentiation, which has been widely applied in water body detection and coastline extraction (Günen and Atasever, 2024). Coastlines for each year were extracted from the MNDWI images with thresholds determined using the method from Otsu (1975). Otsu's method can automatically select the optimal value between the two peaks (water and land in our study) in the histogram of a greyscale image, which has been widely used in image segmentation (Ciecholewski, 2024; Zhou et al., 2023).

After extracting coastlines between 2016 and 2023, the linear regression rate (LRR) method was used to determine the change rate of coastline. Firstly, we generated a reference by sampling the 2023 MSI-derived coastline to points with a 100 m interval. Then, for each point in the reference, we calculated the shortest distance between the point and the coastlines in other years (i.e., 2016 to 2022). Finally, a linear regression analysis was carried out between the time (years) and the calculated shortest distances for each point, and the slope of the regression analysis was determined as the coastline change rate (Fig. 2). This resulted in a list of points with 100 m intervals along the Black Sea coast containing positive slopes that correspond to coastline accretion and negative slopes indicating erosion.

2.2.2. SAR image processing

Sentinel-1 C-band VH-polarized images in July and August between 2016 and 2023 within the 1 km buffer zone were downloaded from the GEE platform. All VH images were pre-processed including thermal noise removal, radiometric calibration and terrain correction, and resampled to 20 m spatial resolution to match the resolution of MSI data. Similar to MSI image processing, we calculated the median of SAR images in July and August for each year to smoothen out any noise and irrelevant variations (e.g., waves).

To identify change, we initially tried the cumulative sum (CUSUM) method (Ruiz-Ramos et al., 2020). We selected the VH image in 2016 as the reference, and subtract the reference from VH images in other years (2017–2023) to obtain the difference intensity (DI_{2016}, Eq. (2)). The area of accretion was determined as pixels with DI exceeding the 95th percentile of DI (positive values), while areas of erosion were determined as pixels where the DI values lower than the 5th percentile of DI (negative values). However, we found that this approach was not effective in detecting recent-accreted areas. We also tried to use CUSUM method with the VH image in 2023 as reference to obtain DI_{2023} (Eq. (3)), but this led to misdetections of early-eroded area. To solve these problems, we finally used the average of DI_{2016} and DI_{2023} in this study. In fact, this resulted in the use of only VH images in 2016 and 2023, after

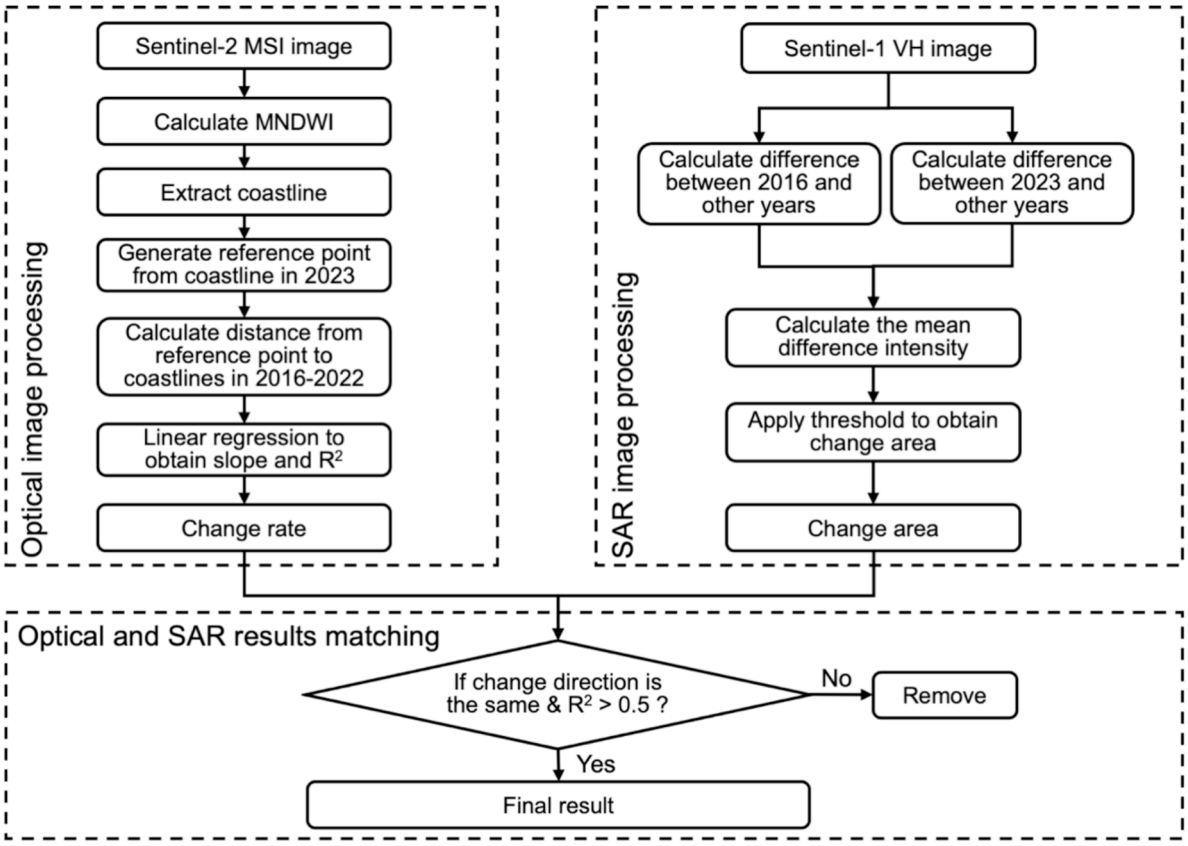

Fig. 2. Data processing workflow for Sentinel-2 MSI and Sentinel-1 SAR images used in this study.

solving Eq. (2) and Eq. (3), but it is more accurate in change area detection compared to using only DI_{2016} or DI_{2023}.

$$DI_{2016} = mean(VH_i - VH_{2016}), i = 2017, \cdots, 2023 \quad (2)$$

$$DI_{2023} = mean(VH_{2023} - VH_j), j = 2016, \cdots, 2022 \quad (3)$$

2.2.3. Combining optical and SAR data

After obtaining the coastline change rate from MSI data and change area from SAR data, we developed an approach to match the two results. Firstly, we calculated the approximate envelope of change during the study period for each point in the MSI result. The approximate envelope is defined as the absolute value of change rate multiplied by the number of years (i.e., 8), and a square buffer surrounding each point of the MSI result was then created. We then investigated the result from SAR within this envelope area (i.e., square buffer), and compared it with the MSI result. If the change direction (erosion or accretion) within this area was the same in both MSI and SAR results, and the determine coefficient of linear regression in MSI data processing (section 2.2.1) was higher than 0.5 (i.e., $R^2 > 0.5$), we considered this area has significantly changed from 2016 to 2023, otherwise it was excluded from the results (Fig. 2). This matching procedure can largely remove false detections due to waves or land cover changes in the SAR results. It can also remove minor changes that are within the error margin of the MSI-derived coastlines. More importantly, it is a way of synergistic use and cross validation between the SAR and MSI results, ensuring the detected results are significant changes.

After matching the MSI and SAR results, we visually inspected each area where coastline change between 2016 and 2023 was detected with the reference from the Google Earth high resolution images, to assess the type of changes. Changes were classified into three categories: natural, artificial, and other changes. Natural changes are changes primarily due to natural processes including fluvio-marine dynamics in deltas and estuaries along the Black Sea, changes to sedimentation patterns along sandy coasts, including due to the impact of energetic waves and nearshore currents. Artificial changes are those that result from direct human activities on the coast, such as the construction of jetties, groynes or seawalls, harbours and other port infrastructures, land reclamation for airports and other engineering structures. Other changes are classified as areas where changes are temporary in nature, mainly because of boat or ship movement, land cover changes and other episodic occurrences.

2.3. *In situ* data collection and validation

In order to validate the coastlines derived from MSI images, we used *in situ*-measured coastline position data along the Danube Delta on the Romanian coast between 2016 and 2023 (*in situ* coastline 1 in Fig. 1), and from the Rioni River mouth on the Georgian coast in 2020 and 2023 (*in situ* coastline 2 in Fig. 1). For *in situ* coastline measurements along the Romanian Black Sea shore, a survey-grade Differential Global Navigation Satellite System (DGNSS) was utilised to record coastline coordinates as points at 3-metre intervals, typically during July and August each year. For the *in situ* coastline measurements in Georgia, a DGNSS system operating in Real Time Kinematic (RTK) mode, integrated with the GEO-CORS continuous base station network of Georgia, was used to capture the configuration of the Rioni River mouth, including the coastlines of the northern and southern river branches. Surveys were conducted in May and August, with survey points recorded at intervals of 5 to 10 m. To validate the accuracy of satellite-derived coastlines, we first sampled the MSI-derived coastlines into points with 100 m intervals, and calculated the shortest distance from the points to the *in situ*-measured coastline for each year. Subsequently, we performed a statistical analysis of the errors for each year. To validate the accuracy of MSI-derived coastline change rate, we calculated the change rate using *in situ* coastline based on the same method as MSI-derived change rate

between Sfantu Gheorghe branch of the Danube Delta and the Sahalin Spit in Romania, where *in situ* data were available from all 8 years. Then we compared it with the MSI-derived coastline change rate in the same location. To validate the area where erosion and accretion exist from SAR images, we visually compared the change area detected from SAR with the *in situ* coastlines.

3. Results

3.1. Validation with in situ data

The average difference between *in situ* coastline and MSI-extracted coastline was 11.8 m for all the validation sites in Romania and Georgia (Fig. 3). 88.8 % of the MSI-derived coastline errors were smaller than 20 m (i.e., one pixel in this study). There are a few locations in 2016 and 2020 where the difference between MSI-derived and *in situ*-measured coastlines is considerably larger. Those points are mainly located around the highly dynamic regions at the Sahalin Spit in the Danube Delta. The errors in the MSI-derived coastlines from 2020 to 2023 are overall smaller than those from 2016 to 2019. The differences between the MSI-derived coastline and the *in situ* coastline in Georgia is slightly smaller than those in Romania. These results indicate that the coastlines were accurately derived from MSI images with an average error of around half a pixel.

Two examples of the comparison between satellite-derived coastlines and *in situ*-measured ones in Sahalin Spit are shown in Fig. 4, which is a highly dynamic region in the Danube Delta. The first example (A1) shows an erosion coastline section (Fig. 4b and 4c), and the second example (A2) shows an area of accretion between 2016 and 2023 (Fig. 4d and 4e). In both cases, the satellite-derived coastlines (points) aligned well with the *in situ*-measured coastlines (solid lines).

The coastline change rate ranges from −42 m/year to 110 m/year along the coast from Sf Gheorghe River mouth southward to the end of Sahalin Spit (location is shown Fig. 4a). Extremely high coastline accretion (> 50 m/year) is observed at the end of Sahalin Spit as the blue points shown in Fig. 5. The change rate from satellite-derived coastline agrees very well with the value calculated from *in situ* coastlines with a root mean square error (RMSE) of 1.73 m/year and mean absolute percentage error (MAPE) of 24.40 % (Fig. 5).

When comparing satellite-detected areas of change based on SAR imagery with *in situ*-measured coastlines from different years between 2016 and 2023, there is a good agreement. For example, Fig. 6a shows the example of erosion at Sahalin Spit in the Danube Delta (A1 as in Fig. 4), the eroded area detected from SAR (red pixels) is located in between the two *in situ* coastlines measured in 2016 and 2023. Similarly, Fig. 6b shows an example of accretion at Sahalin Spit (A2 as in Fig. 4), where the detected change area from SAR images (blue pixels) agrees very well with the changes determined from the *in situ* coastlines.

3.2. Coastline change

In total, 35.1 km^2 changes were observed along the entire Black Sea coast from 2016 to 2023, which include 23.9 km^2 (67.9 %) where the coastline advanced and 11.3 km^2 (32.1 %) where it has retreated. When separating the results into different types of change, 54.5 % of them are natural changes due to coastline erosion or accretion, 34.6 % are artificial changes due to construction activities, and 10.9 % are temporary or random errors due to boat/ship movement or land cover changes on adjacent land (Table 1). Among the areas classified as experiencing natural changes, accretion areas evidence a slightly higher value than erosion areas (9.7 km^2 vs 9.4 km^2), but erosion was observed along a longer extent of coastline (101.3 km) than accretion (81.6 km). Unsurprisingly, in areas classified as artificial change, the total area of coastline advance (11.7 km^2) is significantly higher than coastline retreat (0.5 km^2), and this is also the case for the extent of coastline impacted by artificial changes (66.5 km vs 4.4 km for advance and retreat respectively).

Natural coastline changes were mainly observed in four regions: the coast of the Danube Delta in the western Black Sea, Kızılırmak-Yeşilırmak deltas in the southern Black Sea, Chorokhi-Rioni-Kodori river mouths in the eastern Black Sea, and the coast from Dnieper-Bug Estuary to Karkinit Bay in the northern Black Sea (Fig. 7). Most of the natural changes were observed along deltaic and estuarine regions where river mouths connected to the sea, leading to variability in fluvio-marine channels mainly influenced by variability in river flows.

In the Danube Delta region, a total area of 5.4 km^2 has accreted between 2016 and 2023, while 4.4 km^2 of erosion were observed. Along these accretional and erosional areas, the average change rate was + 22.1 m/year and −10.1 m/year, respectively. The largest accretion hotspot during the monitoring period was the southernmost tip of Sahalin Spit in the Danube Delta, with an increase in area of 1.0 km^2 and average change rate of + 64.0 m/year (Fig. 8a-8c). The most significant erosion hotspot was also located at the Sahalin Spit with an eroded area of 0.5 km^2 at an average change rate of −19.3 m/year (A1 in Figs. 4, 6). The Sahalin Spit is highly dynamic, its southern part (A2 in Fig. 4) represents a sink for sediments brought by the Sf Gheorghe branch of the Danube River, which are transported by the longshore drift. However, the middle section of the spit (A1 in Fig. 4) is exposed to erosion driven by wave-induced nearshore currents.

In the Kızılırmak-Yeşilırmak deltas, a total area of 1.4 km^2 of

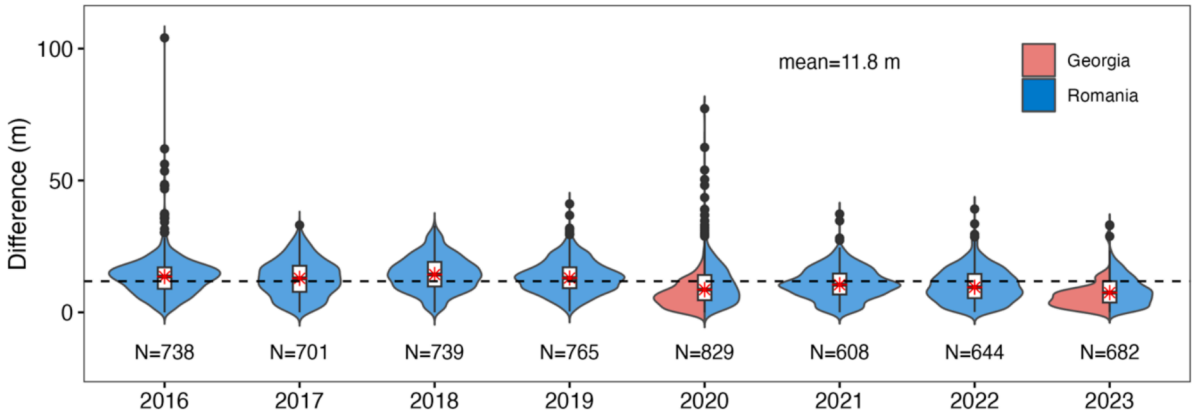

Fig. 3. Difference between *in situ*-measured coastlines and MSI-derived coastlines. Red asterisks represent the median values for data in each year. The upper and lower ends of boxplot represent the 75th and 25th percentiles. The horizontal dashed line indicates the mean difference of data from all eight years. The blue areas represent data from Romania, and red areas represent data from Georgia. (For interpretation of the references to colour in this figure legend, the reader is referred to the web version of this article.)

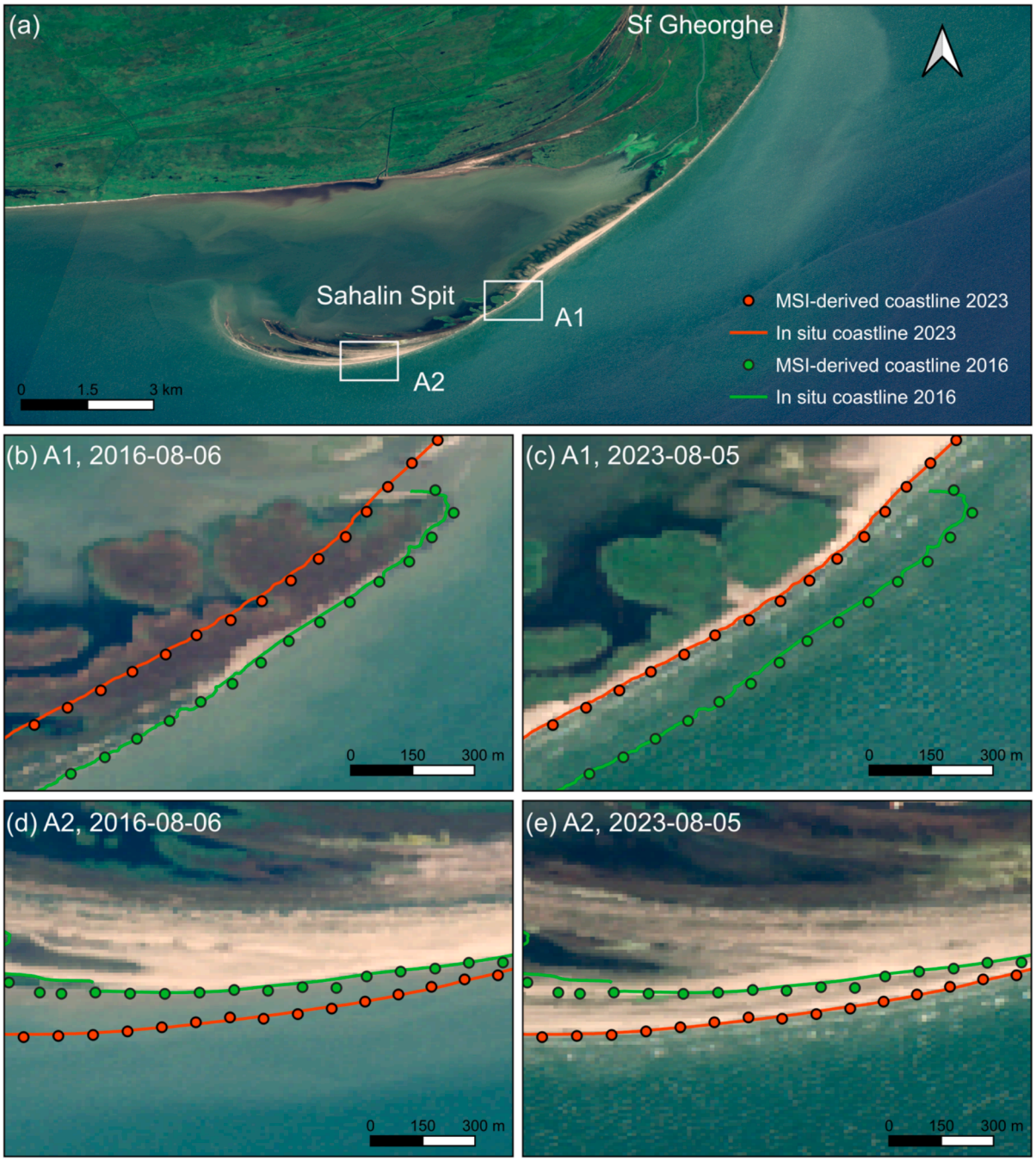

Fig. 4. Examples of comparison between *in situ*-measured coastlines and MSI-derived coastlines in 2016 and 2023 at Sahalin Split in the Danube Delta, Romania. (a) Map of the Sahalin Split. (b) and (c) show an erosional area in the middle of Sahalin Split. (c) and (d) correspond to accretion observed at the tip of Sahalin Split. Background images are from Sentinel-2 MSI true colour imagery.

coastline accretion and 1.3 km^2 of erosion were observed, with an average change rate of + 9.2 m/year and −14.3 m/year, respectively. In terms of hotspots of coastline change, the Yörükler coast experienced accretion of 0.5 km^2 and an average change rate of + 9.6 m/year (Fig. 8d-8f), while erosion was prevalent in the Kızılırmak River Delta near Lake Liman, where the coastline loss 0.7 km^2 with an average change rate of −19.6 m/year (Fig. 8j-8 l). These two locations are geographically very close, and the patterns of coastline change represent the dynamic processes occurring in deltaic systems, where fluvial and marine processes interact leading to episodic deposition of fluvial sediment that is reworked by waves and nearshore currents.

On the Chorokhi-Rioni-Kodori River mouths coast in the eastern Black Sea, a total area of 1.6 km^2 experienced accretion, while 1.8 km^2 were eroded, with average change rates of + 9.6 m/year and −7.9 m/year, respectively. The largest accretional area was located at the north flank of the Rioni River mouth, which has expanded by 0.3 km^2 at an average change rate of + 9.6 m/year (Fig. 8g-8i). The largest erosional hotspot was located along the mouth of the Kodori River channel, where 0.4 km^2 of coastal area was lost, at an average change rate of -41.8 m/year (Fig. 8m-8o). The Kodori River mouth is highly dynamic, and during the monitoring period significant changes of the river channels were observed, with the south channel expanding and the north channel narrowing dramatically (Fig. 8n vs 8o).

Along the coast from Dnieper-Bug Estuary to Karkinit Bay in the north of the Black Sea, coastal changes are characterised by 0.7 km^2 of accretion and 1.1 km^2 of erosion, with average change rates of + 10.9

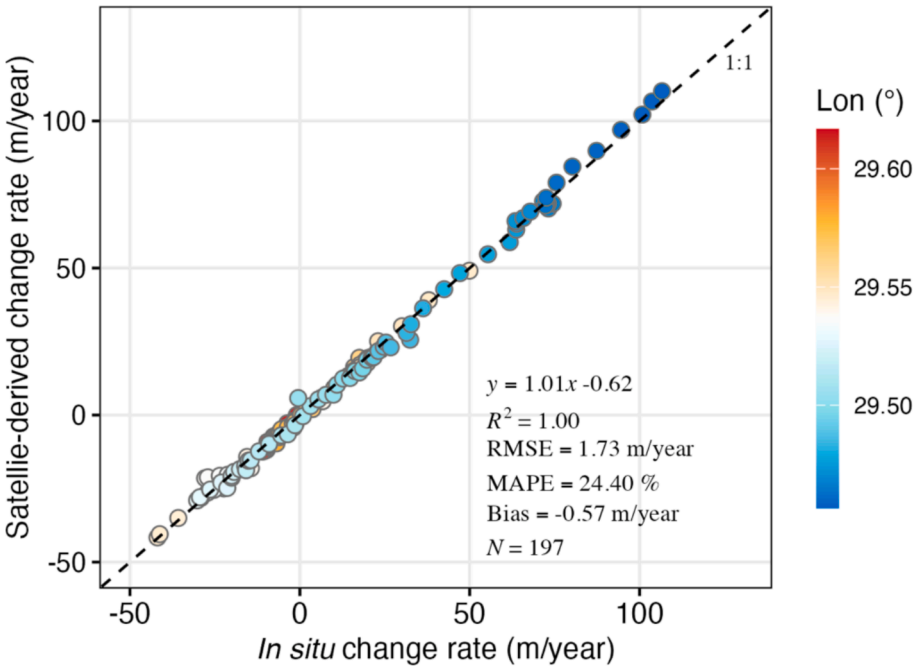

Fig. 5. Comparison of change rates obtained from *in situ* coastline data and MSI-derived coastlines in the region between Sf Gheorghe River mouth and Sahalin Spit in the Danube Delta, colour indicates the longitude.

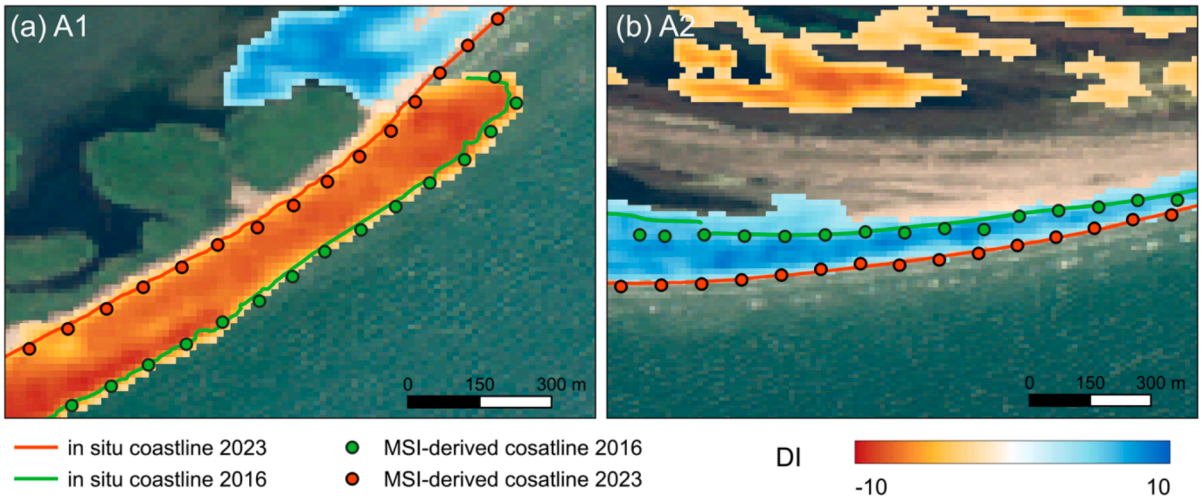

Fig. 6. Comparison of change area detected from SAR images with *in situ*-measured coastlines at Sahalin Spit in the Danube Delta. (a) Erosion case in A1, and (b) accretion case in A2. A1 and A2 are the same locations as in Fig. 4. Background is from the Sentinel-2 MSI true colour image on 5 August 2023. Colour of the pixel represents the difference intensity (DI) from SAR images, where blue indicates accretion and red is erosion. (For interpretation of the references to colour in this figure legend, the reader is referred to the web version of this article.)

Table 1
Summary of coastline changes along the entire Black Sea coast during 2016 and 2023.

Type of change	Direction of change	Area of change (km^2)	Length of change (km)
Natural changes	Accretion	9.7	81.6
Natural changes	Erosion	9.4	101.3
Artificial changes	Advance	11.7	66.5
Artificial changes	Retreat	0.5	4.4
Other changes	All	3.8	21.2

m/year and −6.8 m/year, respectively. Erosion and accretion hotspots are both located at the Gulf of Tendra with equivalent areas of 0.2 km^2, and an average change rate of + 10.6 m/year for accretional areas and −8.9 m/year for erosional areas (Fig. 8p-8r). The coastline is characterised by a very narrow sandy barrier that separates the Gulf of Tendra and the Black Sea.

In terms of artificial changes, which represent 34.6 % of the changed area along the Black Sea coast, 95.8 % of the observed changes correspond to seaward advance of the coastline, and only 4.2 % indicate landward retreat. The vast majority of the observed changes are located along the southern Black Sea coast, with some minor changes on the western and northern coasts (Fig. 9). The top three coastal change hotspots correspond to: (1) the coastal reclamation associated with the construction of Rize-Artvin Airport in eastern Turkey, with the advance

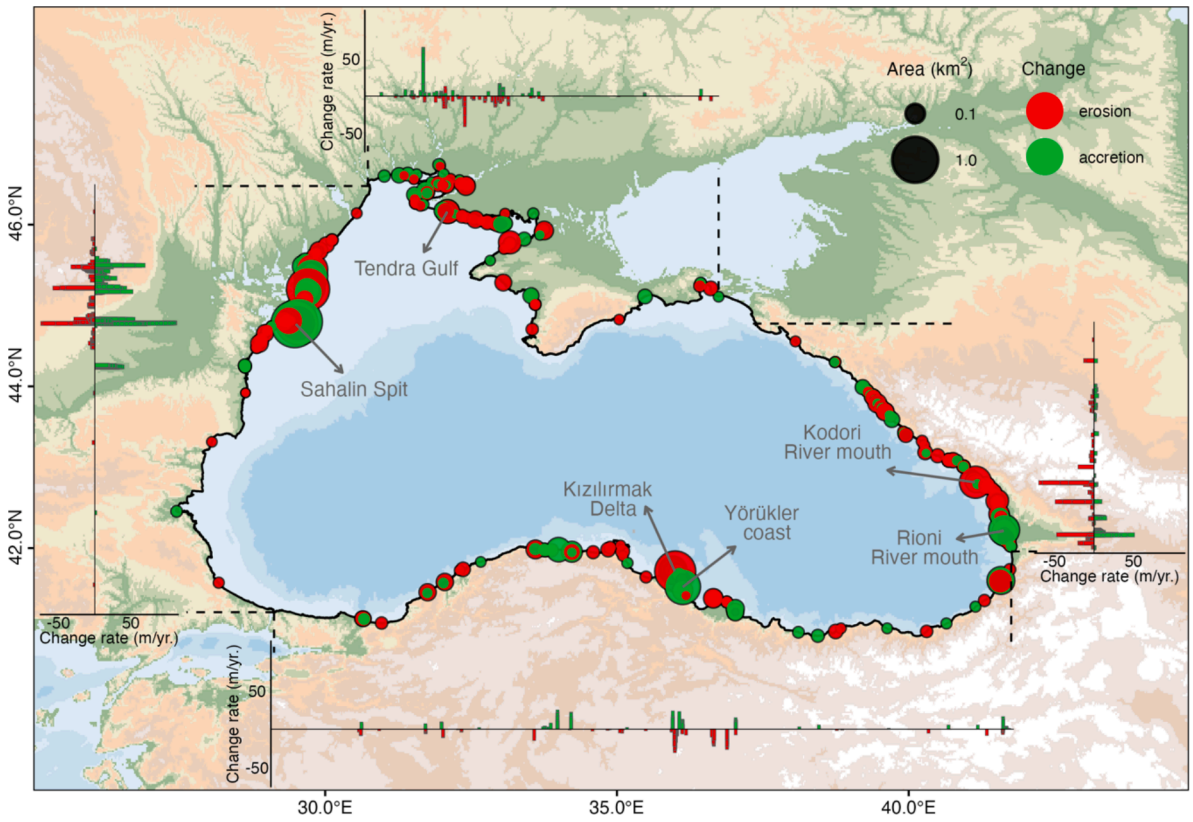

Fig. 7. Natural changes detected from Sentinel-1 SAR and Sentinel-2 MSI images between 2016 and 2023, where the size of the circle represents the area of change, the colour of circle represents the direction of change. Bar graphs show the change rates along the north, west, south and east of the Black Sea coast.

of the coast increasing an area of 2.4 km^2 (Fig. 10a-10c); (2) the reclamation along the coast of Istanbul, which are mostly related to the construction of the Istanbul Airport (Fig. 10d-10f), where several locations experienced coastline advance with the largest two representing an area of 1.9 km^2; (3) the construction of Filyos Port on the south-western coast (Fig. 10g-10i), where coastal advance occurred in an area of 1.1 km^2.

Other changes are mainly noise from boat/ship movement within ports and harbours, as well as land cover changes in land areas adjacent to artificial changes. These are widely distributed along the coast of the entire Black Sea, but are located mainly near cities where intensive human activities exist. Fig. 11 shows an example of detected ship movement in Constanta Port, Romania, between 2016 and 2023.

4. Discussion

4.1. Advantages and limitations of this study

This study developed a new simple approach based on optical and SAR imagery to evaluate coastline change. The accuracy of coastline position extracted from Sentinel-2 MSI images reached around half a pixel (Fig. 3). This confirms that the method proposed in this work can be very useful in coastline monitoring at medium to high spatial resolution across extended regions, especially where *in situ* data are not available. There are two main differences between our method and existing ones. First, in addition to the information (i.e., coastline and change rate) provided by traditional coastline change monitoring methods, our proposed method can directly provide the changed area at the pixel level from SAR data, these information collectively are invaluable for coastal management. Second, the matching procedure between the results from SAR and optical images provides a synergy and cross validation, which increases the robustness of the proposed method and ensures the results of detected changes are reliable. This procedure contributed to largely avoid false detections, such as due to wave-induced variations at the water surface and vegetation changes on adjacent land detected from SAR images, and also cloud patches in optical images.

There is still room for improvement in the proposed method and the results of this work. First, the proposed method didn't consider the influence of tides because it is very small in the Black Sea, which can be ignored when using a 20 m spatial resolution image. Further tests or improvements are needed when applying our method to other regions where the influences of tides cannot be ignored. For example, correcting for the influence of tides by using a tide model and satellite image acquisition time (e.g., Bishop-Taylor et al., 2021). We were not able to detect small coastal changes, especially those at sub-pixel level, because of the spatial resolution (20 m) of the SAR and optical images used in this study. For example, coastline erosion has been observed from field surveys along the southern Romanian Danube Delta coast (near Lake Sinoe), but the sensitivity of the method in this study was insufficient to detect all of those changes. This may have led to some underestimation of coastline change along parts of the Black Sea basin. The spatial resolution of the imagery also contributed to inaccurate coastline delineation in regions where complex coastline features present, such as small jetties and groynes (e.g., Constanta–Tomis Port), small spits (e.g., Prirva River Mouth in the Danube Delta), water bodies close to coast (e.g., Danube Delta, Yahorlyk Bay), wetlands with vegetations and aquatic plants (e.g., Musra Bay in the Danube Delta, Dnipro River mouth). Those inaccuracies in coastline identification have, for sure, generated inaccurate shoreline change metrics in some sectors. Using higher spatial resolution satellite images could address this problem in future studies. River mouths and associated spits are highly dynamic, which adds to the uncertainty of the analysis. For example, the southern tip of Sahalin Spit in the Danube Delta has been subject to complex dynamics because of sediments supplied through the Sf Gheorghe channel and the southward-directed longshore drift (Giosan et al., 1999). Whilst the entire spit has

Fig. 8. Examples of natural changes along the Black Sea from 2016 to 2023. Accretions at (a)-(c) Sahalin Spit in the Danube Delta, (d)-(f) Yörükler coast in Turkey, (g)-(i) Rioni River mouth in Georgia. Erosions in (j)-(l) Kızılırmak Delta in Turkey, (m)-(o) Kodori River mouth in Georgia, (p)-(r) Tendra Gulf in Ukraine. Pixel colour scale represents the difference intensity (DI) from SAR images, where blue indicates accretion and red represents erosion. Background images are from Sentinel-2 MSI true colour imagery. (For interpretation of the references to colour in this figure legend, the reader is referred to the web version of this article.)

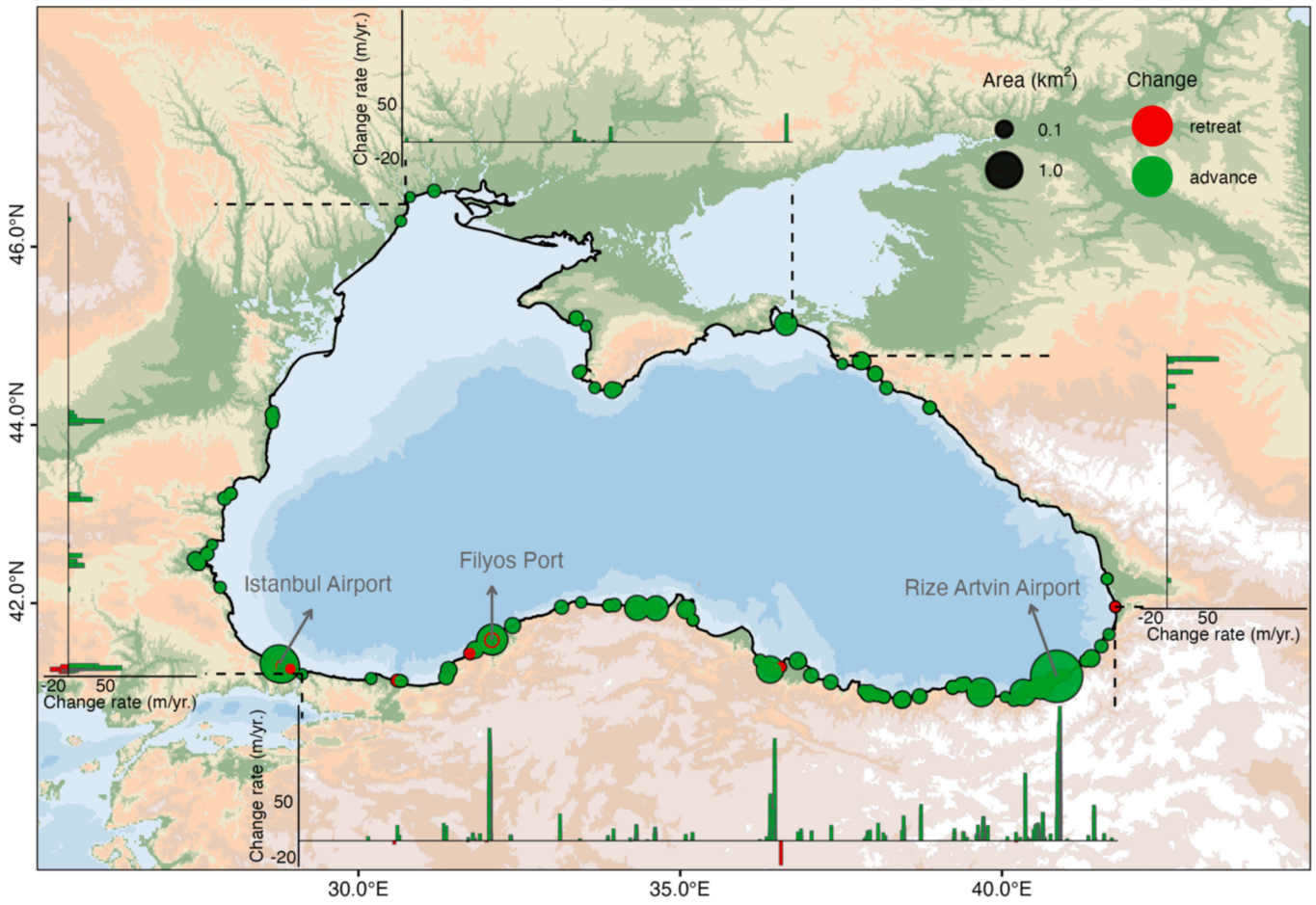

Fig. 9. Artificial changes detected from Sentinel-1 SAR and Sentinel-2 MSI images between 2016 and 2023, where the size of circle represents the area of change, the colour of the circle represents the direction of change. Bar graphs show the change rate along the north, west, south and east of the Black Sea coast.

been moving south-westerly, simple linear erosion and accretion of the southern tip were not able to comprehensively describe the whole coastal change processes. Developing a new approach in the future combining optical and SAR images to detect changes at a higher temporal resolution may help to reconstruct the whole movement of the spit, and improve the coastal dynamics monitoring results.

Our method and the thresholds we used were primarily determined through trials and tests on the Romanian coast, where we have extensive *in situ* data. Although the applications to the entire Black Sea coast showed an overall good accuracy, a few disagreements between SAR-detected changes and MSI-detected changes were found in the results. The first case is in regions where the coast is characterised by flat and bare land. In those regions, the backscattering from the bare land is very low, with SAR processing overestimating the change areas due to the inclusion of nearby areas where vegetation was observed. For example, on the Yörükler coast (Fig. 8d), the area of accretion detected from the SAR imagery included some of the vegetation expansion area. The second case is associated with the fixed percentiles of DI (i.e., 5 % and 95 %) for erosion/accretion detection from SAR. It may have led to underestimation or overestimation in regions where the number of pixels of coastline change are significantly different from those in our test regions. For instance, some pixels of the airport were missed in the SAR detected changes in Fig. 10a, which may because the threshold of 95 % is too high. Developing a method to determine dynamical percentiles as thresholds for different sections of the coast may improve results in the future. Further studies are needed to quantify the accuracy of the estimated surface area of the change detected from SAR images, and to develop a propagation method for quantifying the uncertainties in the final results. In addition, difficulties existed in classifying natural and artificial changes, especially for beaches impacted by human activities. This concluded, for example, the accretion in several beaches on the Romanian coast near Constanta, which are actually the result of a major artificial beach nourishment project that started in 2015. Other examples of human-induced beach accretion observed along the eastern Black Sea coast are related to the construction of groynes.

4.2. *Comparison with reported coastline changes in the Black Sea*

In this study, we observed extensive erosion in the Danube Delta, Yeşilırmak Delta, and along the coast from Dnieper–Bug Estuary to Karkinit Bay, located along the west, south and north of the Black Sea coast, respectively (Fig. 7). Our results from the period between 2016 and 2023 are in line with Görmüş et al. (2021), who also showed erosion in the same regions but for the period between 1972 and 2018. In addition, our results indicate severe erosion in the Kızılırmak Delta and Chorokhi-Rioni-Kodori River mouths, located along the southern and eastern Black Sea coast, respectively. These regions are highly dynamic due to river inflows and sedimentary dynamics in the fluvial-marine interface. In the north-western Black Sea, the coastal change patterns reported here agree with the results from Cherkez et al. (2020), with both studies demonstrating that the largest coastline changes in the north-western Black Sea occur along the Danube Delta, with accretion hotspots along the coast between Musura Bay and Solonyi Kut Gulf, and erosion hotspots in the vicinity of river mouths, especially the Ochakivs'ke River mouth.

On the northern Bulgarian coast, our results do not point to

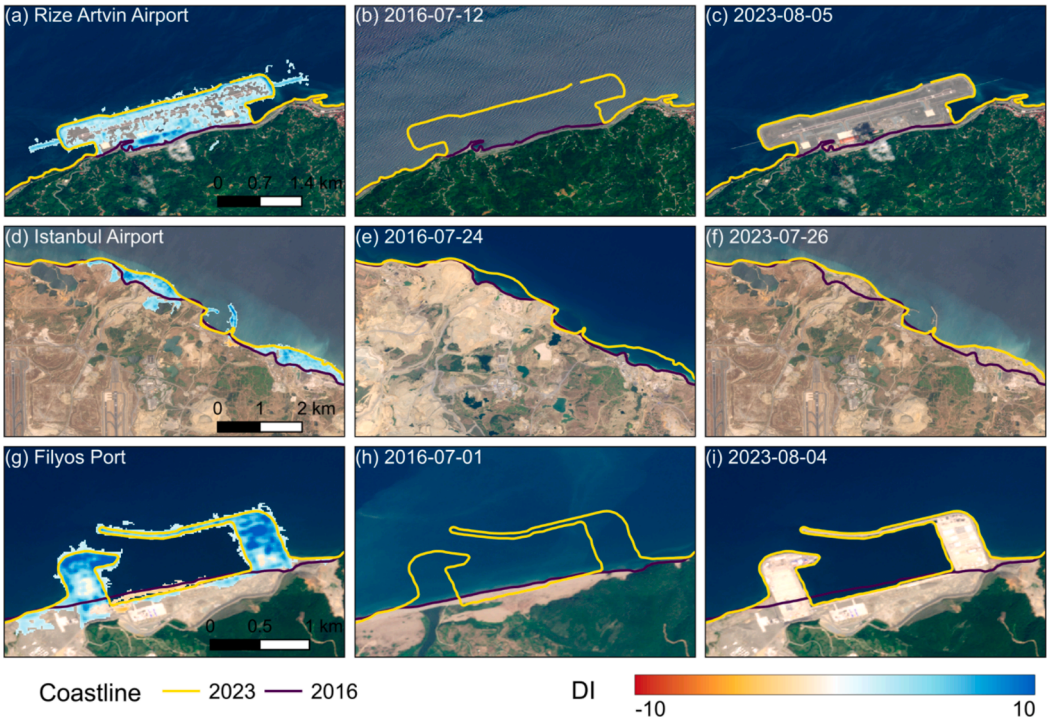

Fig. 10. Examples of artificial changes along the Black Sea from 2016 to 2023. (a)-(c) Rize-Artvin Airport on the eastern Turkey coast, (d)-(f) reclamation along the Istanbul coast, (g)-(i) Filyos Port on the western Turkey coast. Pixel colour scale represents the difference intensity (DI) from SAR images, where blue indicates accretion and red represents erosion. Background images are from Sentinel-2 MSI true colour imagery. (For interpretation of the references to colour in this figure legend, the reader is referred to the web version of this article.)

Fig. 11. An example of ship movement detected in Constanta Port (Romania) during 2016 and 2023. Pixel colour scale represents the difference intensity (DI) from SAR images, where blue indicates accretion and red represents erosion. Background images are from Sentinel-2 MSI true colour imagery. (For interpretation of the references to colour in this figure legend, the reader is referred to the web version of this article.)

significant coastline changes between 2016 and 2023, despite previous work by Stanchev et al. (2018) indicating relevant coastline changes in Bulgaria between 1972 and 2011 based on *in situ* coastline data, topographic maps, and very high resolution orthophoto images. This is likely due to the fact that change rates during the 8-year study period of this work are smaller, and within the error margin due to the 20 m resolution satellite images we used to capture these changes. On the other hand, we observed significant coastline changes near Istanbul Airport between 2016 and 2023 (Fig. 10d-10f), which agrees well with the results from Goksel et al. (2020), who also reported that the main changes along the Istanbul coast between 2009 and 2016 are related to the construction of Istanbul Airport. The construction started in 2014 and finished in 2018 (Tanrıverdi and Lezki, 2021), covering the period of both studies.

In the Yeşilırmak Delta in the south of the Black Sea, our results indicate erosion, which is similar to the changes in coastline position identified by Kuleli et al. (2011) and Kale et al. (2019). Coastline erosion in this area is likely due to the decrease of fluvial sediments supply due to construction of dams along the river catchment (Kale et al., 2019). In the Kızılırmak Delta, we did not observe significant erosion at the eastern flank of Kızılırmak Delta as reported by Kuleli et al. (2011) and Ozturk and Sesli (2015). This is likely due to the construction of a groyne field (top left coast in Fig. 8j) along the coast, which have stopped the erosion in our study period. However, we observed severe erosion along the coast adjacent to Lake Liman (Fig. 8j-8 l), which is located approximately 3 km from the Kızılırmak River mouth, and there is no groyne constructed along the coast. The erosion close to Lake Liman is appears to also be related dam construction across the river catchment (Ozturk and Sesli, 2015).

Although the monitoring period of our study is different from previous studies, as highlighted above, the overall agreement in terms of coastline change hotspots indicates the locations that are most vulnerable to coastal changes along the Black Sea at both interannual and decadal timescales. This provides information required for implementing site-specific coastline monitoring programmes and more detailed studies, while also assisting in the definition of coastal zone management measures.

4.3. Implications for shoreline management

The natural coastline changes from 2016 to 2023 determined in this study are mainly concentrated along the Danube Delta, the Kızılırmak-Yeşilırmak deltas, the Chorokhi-Rioni-Kodori River mouths, and the coast from Dnieper–Bug Estuary to Karkinit Bay. These findings align closely with the spatial distribution of coastal slope and shoreline types (sands, sand with pebbles, sandy-aleuritic) reported by Tătui et al. (2019), which indicate that sedimentary coastlines composed of sand are more susceptible to erosion compared to rocky and other types of shorelines. These change areas also correspond to the main river mouths, which supports the findings from Panin (2005) that the most vulnerable coasts in the Black Sea are characterised as being low-lying and accumulative type. The more stable coastlines according to our results are the cliffs along mountainous areas in the south-western, south-eastern, and northern Black Sea, which also matches with the distribution of coastal hard rocks, sedimentary rocks and moldy rocks from Tătui et al. (2019). Those results confirm that coastline changes are highly related to shoreline types along the Black Sea coast.

We observed 12.2 km^2 of artificial changes along the Black Sea coast between 2016 and 2023, which corresponds to 34.6 % of the total changes across the basin. Most artificial changes are located on the southern coast of the Black Sea (Table 1). This indicates a considerable expansion of human activities in the past eight years, especially along the Turkish coast. From all artificial changes, 95.8 % consists of seaward advance of the coastline, primarily due to the development of airports, ports, harbours, and jetties (e.g., Fig. 10). These construction activities have considerably altered the geomorphological characteristics of the coast, influenced the nearshore current field, and impacted the natural coastal change processes. The long-known effect of such artificial structures on coastal sediment transport, with neighbouring updrift areas experiencing accretion and downdrift areas subjected to accelerated erosion has been extensively identified (Stanica et al., 2007). In addition, pollutions such as noise, hydrocarbon spills, and disposal of construction materials is likely to have occurred. All of those impacts represent threats to the coastal habitats and aquatic animals, and influenced their distributions. Appropriate management strategies are needed to minimise those impacts.

Recently, there has been a shift towards the study and implementation of green or environmentally-friendly measures (nature-based) over traditional grey infrastructure to address coastal erosion (Morris et al., 2018; Singhvi et al., 2022). However, both types of measures bring their own advantages and limitations. It is important to conduct thorough site assessments to evaluate the unique needs of each location and balance the pros and cons of each approach to develop an effective and sustainable coastal defence strategy. The coastal management strategies traditionally put in balance the costs and benefits of each of the coastal protection strategies (Văidianu et al., 2020). The main problem in choosing the proper policy is generally the lack of detailed coastal dynamics information for longer periods of time. Hence, an accurate EO approach, which can properly capture the longer term but also short term (e.g., storm related) dynamics of the beaches and shoreline positions, is critical to support the selection of the proper coastal protection policies especially in parts of the world where historical data are scarce or missing.

The methods outlined and the approaches and tools developed in this study would also be an indispensable contribution to the national methodologies for the assessment of hydromorphological status, such as the ones proposed for Georgia (Gvilava and Savaneli, 2024a, 2024b), and concerned with the pilot location considered in this paper. These methodologies would particularly benefit from integrating *in situ* measurements with EO data to achieve a more comprehensive understanding of hydromorphological dynamics in the Black Sea region.

5. Conclusions

This study confirmed the important potential of Earth Observation for coastline change detection, being especially helpful for large scale monitoring in data poor areas of the Black Sea or where *in situ* monitoring is not possible. Our extensive validation confirmed that the combination of MNDWI with Otsu's thresholding method can efficiently extract accurate coastlines from optical satellite imagery. SAR imagery presented its good capability in change area detection after simply calculating image difference between years. The combining approach proposed in the study can effectively exclude remaining irrelevant noise from SAR data due mainly to waves and land cover changes, and insignificant/temporal changes detected from optical images. Future directions by considering tides, avoiding influence from vegetation changes nearby water, and using higher spatial resolution satellite data can further improve our proposed method and widen its applicability.

In the Black Sea, we observed accretion and erosion primarily occurring along deltaic and estuarine systems where the shorelines are predominantly sandy. Artificial changes represent roughly a third of the coastline change along the Black Sea from 2016 to 2023, and have been mainly observed along the Turkish coast. These results provided useful information for coastal zone management in the Black Sea countries, and help to prioritize locations where further studies or measures need to be taken. We recommend undertaking comprehensive studies at erosional hotspots to identify the most appropriate and effective coastal protection measures for each specific area. Such studies should assess local conditions and needs to determine which strategies, whether involving structural solutions or more natural approaches, are best suited to mitigate erosion. Furthermore, coastal zone management should be addressed not only from a local perspective but also on a broader regional scale. This larger-scale approach ensures that strategies are coordinated and integrated across different areas, enhancing overall effectiveness and resilience in managing coastal erosion throughout the Black Sea region.

CRediT authorship contribution statement

Dalin Jiang: Writing – original draft, Methodology, Investigation, Formal analysis, Data curation, Conceptualization. **Armando Marino:** Writing – review & editing, Methodology, Investigation, Conceptualization. **Maria Ionescu:** Writing – original draft, Investigation, Data curation. **Mamuka Gvilava:** Writing – review & editing, Data curation. **Zura Savaneli:** Writing – review & editing, Data curation. **Carlos Loureiro:** Writing – review & editing, Investigation. **Evangelos Spyrakos:** Writing – review & editing. **Andrew Tyler:** Writing – review & editing, Funding acquisition, Conceptualization. **Adrian Stanica:** Writing – original draft, Investigation, Funding acquisition.

Declaration of competing interest

The authors declare that they have no known competing financial interests or personal relationships that could have appeared to influence the work reported in this paper.

Acknowledgements

This research was supported by the European Union Horizon 2020 DOORS project (Developing Optimal and Open Research Support for the Black Sea, No 101000518). All the shoreline and other geomorphological measurements used to calibrate the EO on the Romanian coast were made using national funds (Core Programmes PN 19-20 and PN 23-30 funded by the Romanian Ministry for Research, Innovation and Digitalization). C. Loureiro acknowledges funding from FCT under contract CEECINST/00052/2021/CP2792/CT0011(https://doi.org/10.54499/CEECINST/00052/2021/CP2792/CT0011) and projects LA/P/00069/2020 granted to the Associate Laboratory ARNET and UID/00350/2020

to CIMA-UALG. We thank the European Space Agency (ESA) for providing and Google Earth Engine platform for accessing the Sentinel-1 SAR and Sentinel-2 MSI images. We thank the editorial team for their time and efforts, and the reviewers for their valuable comments and suggestions.

Data availability

Data will be made available on request.

References

Abaza, V., Antonidze, E., Ikonomov, L., Gvilava, M., Ispas-Sava, C., Yarmak, L., Sahin Hamamci, N., Karamushka, V., Breton, F., Škaričić, Ž., Shipman, B., Özhan, E., 2011. Taking the stock of and advising the way forward with ICZM in the Black Sea region. In: In: Proceedings of the 10th MEDCOAST Conference, pp. 1–11.

Allenbach, K., Garonna, I., Herold, C., Monioudi, I., Giuliani, G., Lehmann, A., Velegrakis, A.F., 2015. Black Sea beaches vulnerability to sea level rise. *Environ. Sci. Policy* 46, 95–109.

Apostolopoulos, D., Nikolakopoulos, K., 2021. A review and meta-analysis of remote sensing data, GIS methods, materials and indices used for monitoring the coastline evolution over the last twenty years. *Eur. J. Remote Sens.* 54 (1), 240–265.

Avşar, N.B., Kutoğlu, Ş.H., 2020. Recent sea level change in the Black Sea from satellite altimetry and tide gauge observations. ISPRS Int. J. Geo Inf. 9 (3), 185.

Aydoğan, B., Ayat, B., 2018. Spatial variability of long-term trends of significant wave heights in the Black Sea. *Appl. Ocean Res.* 79, 20–35.

Bar, B., Swain, R., Das, P., Sahoo, J., Das, D.N., 2024. Spatial analysis and forecasting of coastal dynamics using optical and SAR imageries: A case study of Contai coastal tract of bay of Bengal. *J. Indian Soc. Remote Sens.* 1–24.

Barbier, E.B., Hacker, S.D., Kennedy, C., Koch, E.W., Stier, A.C., Silliman, B.R., 2011. The value of estuarine and coastal ecosystem services. Ecol. Monogr. 81 (2), 169–193.

Bishop-Taylor, R., Nanson, R., Sagar, S., Lymburner, L., 2021. Mapping Australia's dynamic coastline at mean sea level using three decades of Landsat imagery. *Remote Sens. Environ.* 267, 112734.

Cherkez, E. A., Medinets, V. I., Pavlik, T. V., Gazyetov, Y. I., Medinets, S. V., & Kozlova, T. V. (2020). Using of Landsat space images to study the dynamic of coastline changes in the Black Sea north-western part in 1983–2013. In Geoinformatics: Theoretical and Applied Aspects 2020 (Vol. 2020, No. 1, pp. 1-5). European Association of Geoscientists & Engineers.

Ciecholewski, M., 2024. Review of Segmentation Methods for Coastline Detection in SAR Images. *Arch. Comput. Meth. Eng.* 31 (2), 839–869.

Cohen, J.E., Small, C., Mellinger, A., Gallup, J., Sachs, J., 1997. Estimates of coastal populations. *Science* 278 (5341), 1209–1213.

Edmonds, D.A., Caldwell, R.L., Brondizio, E.S., Siani, S.M., 2020. Coastal flooding will disproportionately impact people on river deltas. *Nat. Commun.* 11 (1), 4741.

Feyisa, G.L., Meilby, H., Fensholt, R., Proud, S.R., 2014. Automated Water Extraction Index: A new technique for surface water mapping using Landsat imagery. *Remote Sens. Environ.* 140, 23–35.

Fogarin, S., Zanetti, M., Dal Barco, M.K., Zennaro, F., Furlan, E., Torresan, S., Critto, A., 2023. Combining remote sensing analysis with machine learning to evaluate short-term coastal evolution trend in the shoreline of Venice. *Sci. Total Environ.* 859, 160293.

Ghosh, M.K., Kumar, L., Roy, C., 2015. Monitoring the coastline change of Hatiya Island in Bangladesh using remote sensing techniques. *ISPRS J. Photogramm. Remote Sens.* 101, 137–144.

Giosan, L., Bokuniewicz, H., Panin, N., Postolache, I., 1999. Longshore sediment transport pattern along the Romanian Danube delta coast. *J. Coast. Res.* 859–871.

Goksel, C., Senel, G., Dogru, A.O., 2020. Determination of shoreline change along the Black Sea coast of Istanbul using remote sensing and GIS technology. *Desalin. Water Treat.* 177, 242–247.

Görmüş, T., Ayat, B., Aydoğan, B., Tătui, F., 2021. Basin scale spatiotemporal analysis of shoreline change in the Black Sea. *Estuar. Coast. Shelf Sci.* 252, 107247.

Günen, M.A., Atasever, U.H., 2024. Remote sensing and monitoring of water resources: A comparative study of different indices and thresholding methods. *Sci. Total Environ.* 926, 172117.

Gvilava, M., and Savaneli, Z. (2024a). Proposal of a National Methodology for the Assessment of the HydroMorphological Status of the Black Sea Coastal and Transitional Water Bodies in Georgia. Tbilisi, Georgia, March 2024. EU4Environment - Water & Data Consortium, Umweltbundesamt GmbH, Austria, and IOW, France.

Gvilava, M., and Savaneli, Z. (2024b). Proposal of a National Methodology for the Assessment of the HydroMorphological Status of the Black Sea Coastal and Transitional Water Bodies in Georgia: Poti Area Application. Tbilisi, Georgia, May 2024. EU4Environment - Water & Data Consortium, Umweltbundesamt GmbH, Austria, and IOW, France.

Halcrow U.K., GeoEcoMar, NIMRD 'Antipa', University of Bucharest, ISMAR-CNR., 2012. 'Master Plan for the Protection against erosion and Rehabilitation of the Romanian coastal zone'.

Hauer, M.E., Fussell, E., Mueller, V., Burkett, M., Call, M., Abel, K., Wrathall, D., 2020. Sea-level rise and human migration. *Nat. Rev. Earth Environ.* 1 (1), 28–39.

Hooijer, A., Vernimmen, R., 2021. Global LiDAR land elevation data reveal greatest sea-level rise vulnerability in the tropics. *Nat. Commun.* 12 (1), 3592.

Ipcc, 2021. Summary for Policymakers. Climate Change 2021: the Physical Science Basis. Contribution of Working Group I to the Sixth Assessment Report of the Intergovernmental Panel on Climate Change. In press.

Jiang, D., Scholze, J., Liu, X., Simis, S.G., Stelzer, K., Müller, D., Spyrakos, E., 2023. A data-driven approach to flag land-affected signals in satellite derived water quality from small lakes. *Int. J. Appl. Earth Observat. Geoinformat.* 117, 103188.

Kale, M.M., Ataol, M., Tekkanat, I.S., 2019. Assessment of shoreline alterations using a Digital Shoreline Analysis System: a case study of changes in the Yeşilırmak Delta in northern Turkey from 1953 to 2017. *Environ. Monit. Assess.* 191, 1–13.

Karsli, F., Guneroglu, A., Dihkan, M., 2011. Spatio-temporal shoreline changes along the southern Black Sea coastal zone. *J. Appl. Remote Sens.* 5 (1), 053545.

Kosyan, R.D., Velikova, V.N., 2016. Coastal zone–Terra (and aqua) incognita–Integrated coastal zone management in the Black Sea. *Estuar. Coast. Shelf Sci.* 169, A1–A16.

Kuleli, T., Guneroglu, A., Karsli, F., Dihkan, M., 2011. Automatic detection of shoreline change on coastal Ramsar wetlands of Turkey. *Ocean Eng.* 38 (10), 1141–1149.

Lehner, B., Verdin, K., Jarvis, A.(2008). New global hydrography derived from spaceborneelevation data. Eos, Transactions, 89(10): 93-94. Data available at https://www.hydrosheds.org.

Luijendijk, A., Hagenaars, G., Ranasinghe, R., Baart, F., Donchyts, G., Aarninkhof, S., 2018. The state of the world's beaches. *Sci. Rep.* 8 (1), 1–11.

Luisetti, T., Turner, R.K., Jickells, T., Andrews, J., Elliott, M., Schaafsma, M., Watts, W., 2014. Coastal Zone Ecosystem Services: From science to values and decision making; a case study. *Sci. Total Environ.* 493, 682–693.

Mao, Y., Splinter, K.D., 2025. Application of SAR-Optical fusion to extract shoreline position from Cloud-Contaminated satellite images. *ISPRS J. Photogramm. Remote Sens.* 220, 563–579.

McLean, R.F., Tsyban, A., Burkett, V., Codignotto, J.O., Forbes, D.L., Mimura, N., Ittekkot, V., 2001. Coastal zones and marine ecosystems. *Clim. Change* 343–379.

Medinets, V. I., Cherkez, E. A., Pavlik, T. V., Shatalin, S. M., Kozlova, T. V., Kuzmenko, A. Y., ... & Soltys, I. E. (2022). Long-term changes of the shoreline dynamics in the Ukrainian North-Western Black Sea during 1980–2020. In 16th International Conference Monitoring of Geological Processes and Ecological Condition of the Environment (Vol. 2022, No. 1, pp. 1-5). European Association of Geoscientists & Engineers.

Mentaschi, L., Vousdoukas, M.I., Pekel, J.F., Voukouvalas, E., Feyen, L., 2018. Global long-term observations of coastal erosion and accretion. *Sci. Rep.* 8 (1), 12876.

Michener, W.K., Blood, E.R., Bildstein, K.L., Brinson, M.M., Gardner, L.R., 1997. Climate change, hurricanes and tropical storms, and rising sea level in coastal wetlands. *Ecol. Appl.* 7 (3), 770–801.

Modava, M., Akbarizadeh, G., Soroosh, M., 2018. Integration of spectral histogram and level set for coastline detection in SAR images. *IEEE Trans. Aerosp. Electron. Syst.* 55 (2), 810–819.

Morris, R.L., Konlechner, T.M., Ghisalberti, M., Swearer, S.E., 2018. From grey to green: Efficacy of eco-engineering solutions for nature-based coastal defence. *Glob. Chang. Biol.* 24 (5), 1827–1842.

Newton, A., Brito, A.C., Icely, J.D., Derolez, V., Clara, I., Angus, S., Khokhlov, V., 2018. Assessing, quantifying and valuing the ecosystem services of coastal lagoons. *J. Nat. Conserv.* 44, 50–65.

Nicholls, R.J., Cazenave, A., 2010. Sea-level rise and its impact on coastal zones. *Science* 328 (5985), 1517–1520.

Nicholls, R.J., Lincke, D., Hinkel, J., Brown, S., Vafeidis, A.T., Meyssignac, B., Fang, J., 2021. A global analysis of subsidence, relative sea-level change and coastal flood exposure. *Nat. Clim. Chang.* 11 (4), 338–342.

Niedermeier, A., Romaneessen, E., Lehner, S., 2000. Detection of coastlines in SAR images using wavelet methods. *IEEE Trans. Geosci. Remote Sens.* 38 (5), 2270–2281.

Otsu, N., 1975. A threshold selection method from gray-level histograms. *Automatica* 11 (285–296), 23–27.

Ozturk, D., Sesli, F.A., 2015. Shoreline change analysis of the Kizilirmak Lagoon Series. *Ocean Coast. Manag.* 118, 290–308.

Panin, N., 2005. The Black Sea coastal zone–an overview. *Geo-Eco-Marina* 11, 21–40.

Panin, N., Jipa, D., 2002. Danube River sediment input and its interaction with the north-western Black Sea. *Estuar. Coast. Shelf Sci.* 54 (3), 551–562.

Paz-Delgado, M.V., Payo, A., Gómez-Pazo, A., Beck, A.L., Savastano, S., 2022. Shoreline Change from Optical and Sar Satellite Imagery at Macro-Tidal Estuarine, Cliffed Open-Coast and Gravel Pocket-Beach Environments. *J. Marine Sci. Eng.* 10 (5), 561.

Ruiz-Ramos, J., Marino, A., Boardman, C., Suarez, J., 2020. Continuous forest monitoring using cumulative sums of sentinel-1 timeseries. *Remote Sens. (Basel)* 12 (18), 3061.

Scala, P., Manno, G., Ciraolo, G., 2024. Semantic segmentation of coastal aerial/satellite images using deep learning techniques: An application to coastline detection. *Comput. Geosci.* 192, 105704.

Seale, C., Redfern, T., Chatfield, P., Luo, C., Dempsey, K., 2022. Coastline detection in satellite imagery: A deep learning approach on new benchmark data. *Remote Sens. Environ.* 278, 113044.

Sekovski, I., Stecchi, F., Mancini, F., Del Rio, L., 2014. Image classification methods applied to shoreline extraction on very high-resolution multispectral imagery. *Int. J. Remote Sens.* 35 (10), 3556–3578.

Singhvi, A., Luijendijk, A.P., van Oudenhoven, A.P., 2022. The grey–green spectrum: A review of coastal protection interventions. *J. Environ. Manage.* 311, 114824.

Stanchev, H., Stancheva, M., Young, R., Palazov, A., 2018. Analysis of shoreline changes and cliff retreat to support Marine Spatial Planning in Shabla Municipality, Northeast Bulgaria. *Ocean Coast. Manag.* 156, 127–140.

Stanica, A., Panin, N., 2009. Present evolution and future predictions for the deltaic coastal zone between the Sulina and Sf. Gheorghe Danube river mouths (Romania). *Geomorphology* 107 (1–2), 41–46.

Stanica, A., Dan, S., Ungureanu, V.G., 2007. Coastal changes at the Sulina mouth of the Danube River as a result of human activities. *Mar. Pollut. Bull.* 55 (10–12), 555–563.
Tanrıverdi, G., Lezki, Ş., 2021. Istanbul Airport (IGA) and quest of best competitive strategy for air cargo carriers in new competition environment: A fuzzy multi-criteria approach. *J. Air Transp. Manag.* 95, 102088.
Tătui, F., Pîrvan, M., Popa, M., Aydogan, B., Ayat, B., Görmüş, T., Saprykina, Y., 2019. The Black Sea coastline erosion: Index-based sensitivity assessment and management-related issues. *Ocean Coast. Manag.* 182, 104949.
Tsokas, A., Rysz, M., Pardalos, P.M., Dipple, K., 2022. SAR data applications in earth observation: An overview. *Expert Syst. Appl.* 205, 117342.
Ungureanu, V.G., Stanica, A., 2000. Impact of human activities on the evolution of the Romanian Black Sea beaches. *Lakes Reserv. Res. Manag.* 5 (2), 111–115.
United Nations Department of Economic and Social Affairs, Population Division (2022). World Population Prospects 2022: Summary of Results. UN DESA/POP/2022/TR/NO. 3.
Văidianu, N., Tătui, F., Ristea, M., Stănică, A., 2020. Managing coastal protection through multi-scale governance structures in Romania. *Mar. Policy* 112, 103567.
Vespremeanu, E., & Golumbeanu, M. (2017). The Black Sea: Physical, Environmental and Historical Perspectives. Springer.
Vilibić, I., Denamiel, C., Zemunik, P., Monserrat, S., 2021. The Mediterranean and Black Sea meteotsunamis: an overview. *Nat. Hazards* 106, 1223–1267.
Vos, K., Harley, M.D., Splinter, K.D., Simmons, J.A., Turner, I.L., 2019. Sub-annual to multi-decadal shoreline variability from publicly available satellite imagery. *Coast. Eng.* 150, 160–174.
Xu, H., 2006. Modification of normalised difference water index (NDWI) to enhance open water features in remotely sensed imagery. *Int. J. Remote Sens.* 27 (14), 3025–3033.
Yasir, M., Liu, S., Pirasteh, S., Xu, M., Sheng, H., Wan, J., Li, J., 2024. YOLOShipTracker: Tracking ships in SAR images using lightweight YOLOv8. *Int. J. Appl. Earth Observat. Geoinformat.* 134, 104137.
Yasir, M., Sheng, H., Fan, H., Nazir, S., Niang, A.J., Salauddin, M., Khan, S., 2020. Automatic coastline extraction and changes analysis using remote sensing and GIS technology. *IEEE Access* 8, 180156–180170.
Zhou, X., Wang, J., Zheng, F., Wang, H., Yang, H., 2023. An Overview of Coastline Extraction from Remote Sensing Data. *Remote Sens. (Basel)* 15 (19), 4865.
Zhu, Q., Li, P., Li, Z., Pu, S., Wu, X., Bi, N., Wang, H., 2021. Spatiotemporal changes of coastline over the Yellow River Delta in the previous 40 years with optical and SAR remote sensing. *Remote Sens. (Basel)* 13 (10), 1940.